International Journal of Greenhouse Gas Control 133 (2024) 104101

Contents lists available at ScienceDirect

International Journal of Greenhouse Gas Control

journal homepage: www.elsevier.com/locate/ijggc

Potential secondary seals within overburden: Observation from the CO_2 storage sites Aurora and Smeaheia, northern North Sea

Md Jamilur Rahman [a,*], Manzar Fawad [b,1], Nazmul Haque Mondol [a,c]

[a] Department of Geosciences, University of Oslo (UiO), Sem Sælands vei 1, 0371, Oslo, Norway
[b] College of Petroleum Engineering & Geosciences, King Fahd University of Petroleum and Minerals (KFUPM), Dhahran 31261, Saudi Arabia
[c] Norwegian Geotechnical Institute (NGI), Sognsveien 72, 0806, Oslo, Norway

ARTICLE INFO

Keywords:
Overburden
Secondary seal
Polygonal faults
CCS
Aurora
Smeaheia
Horda platform
Northern North Sea

ABSTRACT

This study evaluates potential secondary seals within the overburden in two CO_2 storage sites, Aurora and Smeaheia within the Horda Platform area, of the northern North Sea. Secondary sealing intervals provide for safe and reliable CO_2 storage as they prevent injected fluids from migrating into the atmosphere in the case of primary seal failure. This study analyzes the possible fate of the CO_2 plume in the case of primary seal failure for the Aurora and Smeaheia CO_2 storage sites by evaluating the secondary caprock and sealing potential of polygonal fault systems within the overburden intervals using structural reliability methods. Our findings suggest that a ductile secondary caprock is present in the overburden intervals of the storage sites, which could act as a secondary seal in the case of primary seal failure. The trapped hydrocarbon leaked from the Troll field within this ductile unit indicating a good secondary sealing potential. The study also reveals the presence of polygonal fault systems in the entire study area, but their frequency and orientation vary between layers. However, polygonal fault systems are not structurally stable, posing a risk of fault-parallel flow within the overburden interval. Nonetheless, the ductile clay-rich secondary caprock provides a seal for the polygonal fault systems within the interval. Due to either erosion or non-deposition, the ductile rock interval is not present in the east of the study area. As such, the critical risk for the Alpha structure in the Smeaheia injection site is the Vette fault and the efficiency of the primary Draupne caprock. Moreover, the crucial factor in the western Aurora site is the connectivity between the depleted Troll reservoirs and the CO_2-injected pressurized reservoirs underneath. Based on our qualitative assessment, it is concluded that the overburden interval in the Horda Platform has adequate secondary sealing potential to hold and accumulate CO_2 in the case of primary seal failure. Still, further numerical simulations are recommended to quantify our findings for both the Aurora and Smeaheia sites.

1. Introduction

Top seal integrity is critical in hydrocarbon exploration and fluid injection projects such as subsurface CO_2 sequestration, wastewater disposal, nuclear waste disposal, etc. The potential sealing capacity of any caprock can be estimated from the acting forces such as buoyancy and capillary pressure. Caprock failure may occur when the interval's buoyancy force exceeds the capillary entry pressure or fracture pressure (Foschi and Cartwright, 2020; Ingram et al., 1997; Schowalter, 1979). Additionally, subsurface fluid injection (i.e., CO_2 storage, wastewater disposal, hydraulic fracing, etc.) may introduce injection-induced pressure perturbation and seismicity, affecting the seal integrity. If primary seal failure occurs, the injected fluids migrate into the overburden interval. How the leakage of hydrocarbons and other gases occurs and the trace marks it leaves behind have been characterized and modelled in great detail within the literature (Schroot et al., 2005; Yarushina et al., 2020; Johnson et al., 2022c). Fluid leakage pathways, often referred to as gas 'chimneys', can also be easily detectable in seismic sections as a columnar disturbance with lower reflection continuity and amplitudes than the surrounding areas (Foschi and Cartwright, 2020; Heggland, 1997; Sales, 1997). Additionally, the escaped hydrocarbon might migrate through incompetent caprock (Johnson et al., 2022c; Yarushina et al., 2020) or up the seabed, manifesting as pockmarks (offshore site) in case there is no secondary seal within the overburden (Schroot et al.,

* Corresponding author.
E-mail address: m.j.rahman@geo.uio.no (M.J. Rahman).
[1] Former UiO Researcher.

https://doi.org/10.1016/j.ijggc.2024.104101
Received 25 May 2023; Received in revised form 22 January 2024; Accepted 24 February 2024
Available online 6 March 2024

2005). However, the migrated fluids can be trapped in the overburden due to the presence of any effective secondary sealing intervals. Therefore, characterizing the overburden interval is beneficial for the additional safety of any fluid injection project, especially the CO_2 storage site, in case of leakage or failure of the primary seal. Learnings from hydrocarbon-related leakage might be beneficial, but hydrocarbon molecule diffusion into the overlying rocks and the escaping process has been posited by some to be extremely slow (Abay, 2017; Leythaeuser et al., 1984, 1982; Sales, 1997; Smith et al., 1971). Other groups (Panahi et al., 2013; Johnson et al., 2022c; Yarushina et al., 2020) have posited that hydrocarbon transportation could occur comparatively rapidly, controlled by the pressure build up required to open migration pathways. Nonetheless, hydrocarbon escape could provide suitable analogs for qualitative assessment of safe and reliable subsurface fluid storage.

Generally, various rocks of different mechanical properties were deposited as thick overburden, depending on the paleo-depositional settings and regional tectonics. Different diagenesis histories with faults and fractures are also present in the overburden intervals. However, the overburden interval is mostly neglected while acquiring geological and petrophysical data. The anisotropic nature of overburden and the presence of faults in the study area are well known (Rahman et al., 2022a; Md Jamilur 2022d; Wrona et al., 2017). Nonetheless, the overburden interval as a potential secondary seal and the sealing potential of the faults it contains were never assessed with respect to the CO_2 storage sites in the northern North Sea.

This study is an attempt to evaluate the overburden interval for the presence of potential secondary seals (caprock shale and sealing faults) of two CO_2 storage sites, Aurora and Smeaheia, in the northern North Sea. A qualitative assessment of the plume migration within the overburden interval due to possible primary seal failure scenarios has been analyzed. Gas leakage from the Troll field (Rahman et al., 2022b) has been used as an analogue to interpret the fate of the CO_2 plume if the primary seal failed in both the Aurora and Smeaheia CO_2 injection sites. In addition, the sealing potential of the polygonal fault system within the overburden interval has been evaluated using structural reliability methods. Finally, considering different scenarios, critical factors for reliable storage in both sites have been qualitatively assessed.

2. Study area and polygonal fault system

Northern North Sea, especially the Horda Platform (HP) area, will be the initial hub for future subsurface CO_2 storage as the Norwegian Government awarded three CCS licenses here (EL001-Aurora, EL002-Smeaheia & EL004-Luna). Two CO_2 injection wells (31/5-A-7 AH & 31/5-C-1H) within the first exploitation license EL001 (Aurora) have recently been drilled and are expected to become operational soon with a megatonne level of injection (NPD, 2023). This full-scale (capture, transport and storage) demonstration project (called Longship) has been initiated by the Norwegian Government and Northern Light JV (a joint venture company owned by Equinor, Shell, and TotalEnergies). As part of the project plan, CO_2 will be captured from the industrial point source (i.e., cement factory and waste-to-energy plant). Then, it will be liquefied and transported by ships to an onshore terminal (Øygarden municipality) on the Norwegian west coast. From there, through a pipeline (~100 km), the supercritical CO_2 will be injected into the deep saline aquifer. As the Horda Platform area will be the hub, this study characterizes the overburden interval in the injection sites to evaluate possible leakage pathways and secondary seal potential, mainly focusing on two CO_2 storage sites, Aurora (EL001) and Smeaheia (EL002).

The Horda Platform experienced two primary rifting events during the Permo-Triassic and the Late Jurassic to Mid-Cretaceous (Færseth, 1996; Steel and Ryseth, 1990; Whipp et al., 2014). The area became a wide basin with deep-rooted faults during the first rifting event, where thick syn-depositional wedges were deposited. During the second event, major rifting and tilting shifted westward with fewer activities on the Horda Platform (Stewart et al., 1995). However, it is assumed that the Horda Platform experienced weak stretching due to the reactivation of major Permo-Triassic faults (Færseth, 1996; Roberts et al., 1993, 2019; Steel and Ryseth, 1990; Steel, 1993; Whipp et al., 2014). The faults oriented N-S, NE-SW, and NW-SE controlled the basin formation with half-grabens (15–50 km in width) and defined the morphological elements in the area (Færseth, 1996). In the North Sea, there are instances where half-grabens can extend up to 100 km in length along the strike. However, normal faults generally tend to occur in smaller segments with a maximum length of around 20 km each (Jackson and White, 1989; Roberts and Jackson, 1991). These findings have been supported by various studies that have highlighted the significant influence of major and minor faults resulting from rifting and subsequent thermal subsidence (Anell et al., 2009; Faleide et al., 2015; Jordt et al., 1995). These faults have played crucial roles in the region's structural deformation and deposition of sediments.

The studied Aurora and Smeaheia CO_2 storage sites are bounded by five N-S trending major normal faults (Fig. 1a). The Øygarden Fault Complex bounds the Smeaheia area to the east and Vette fault to the west. The Aurora area is located further west, bounded by the Tusse fault to the east and the Svartalv fault to the west (Fig. 1a). The westernmost Troll fault bounds the Horda Platform in the west. The study area is significantly influenced by these structural elements that have controlled the paleo-deposition here. As a result of this, the composition of the facies varies both laterally and vertically. Different reservoir-caprock pairs are targeted to store CO_2 for the Aurora (Lower Jurassic Dunlin Group) and Smeaheia (Upper to Middle Jurassic Viking Group) sites, which are significantly varied both depositionally and diagenetically (Fig. 1b).

The Lower Jurassic Drake formation shales are the primary caprock for the Aurora site that drapes over the reservoir rocks of the Johansen and Cook formation sandstones. The caprock, Drake formation, mainly consists of marine shales (Steel, 1993) within the deeper parts of the sub-basins (Vollset and Doré, 1984). The reservoir rocks, Johansen and Cook formation sandstones of the Aurora site are mainly separated by the upper part of the Amundsen shales and siltstones. However, the Amundsen Formation has not been deposited in the entire region; hence, Johansen and Cook formation sandstones are juxtaposed and treated as one reservoir (Rahman et al., 2022c). The Johansen and Cook formation sandstones have good to moderate reservoir quality, and the total capacity to store CO_2 in the Aurora site depends on the communication between them (Gassnova, 2012; NPD, 2023).

At the Smeaheia site, the primary caprock is formed by the organic-rich Draupne Formation shale, part of the Viking Group, that drapes over a variety of potential reservoir rocks, including the Upper to Middle Jurassic sandstones of the Sognefjord, Fensfjord, and Krossfjord formations. The caprock shale was deposited during the Upper Jurassic period within the East Shetland Basin, the Viking Graben, and over the Horda Platform area (NPD CO2 Atlas, 2014). The deposition of the shale took place in an open marine environment characterized by restricted bottom circulation and frequent anaerobic conditions (NPD, 2023). The shale itself is composed of a dark gray-brown to black claystone, typically non-calcareous, carbonaceous, and occasionally fissile in nature (Johnson et al., 2022b; NPD, 2023; Rahman et al., 2022e). The reservoir sandstones (i.e., Sognefjord, Fensfjord, Krossfjord) exhibit good to moderate reservoir quality (Dreyer et al., 2005; Mondol et al., 2018; Fawad et al., 2021; Holgate et al., 2015). They were deposited in a shallow coastal marine environment and often intermingled with the Heather Formation shale (NPD, 2023).

A thick overburden interval in the study area comprises deposits from the post-rift sag phase, which commenced in the Early Cretaceous. This marked the transition from fault-controlled to thermally controlled subsidence (Faleide et al., 2002; Jordt et al., 2000; Joy, 1993; Kyrkjebø et al., 2001; Wrona et al., 2017). The overburden interval is characterized by the presence of the Shetland, Rogaland, Hordaland, and Nordland Groups (Fig. 1b). These groups were filled with sediments originating from the uplifted basin margin, particularly from the east

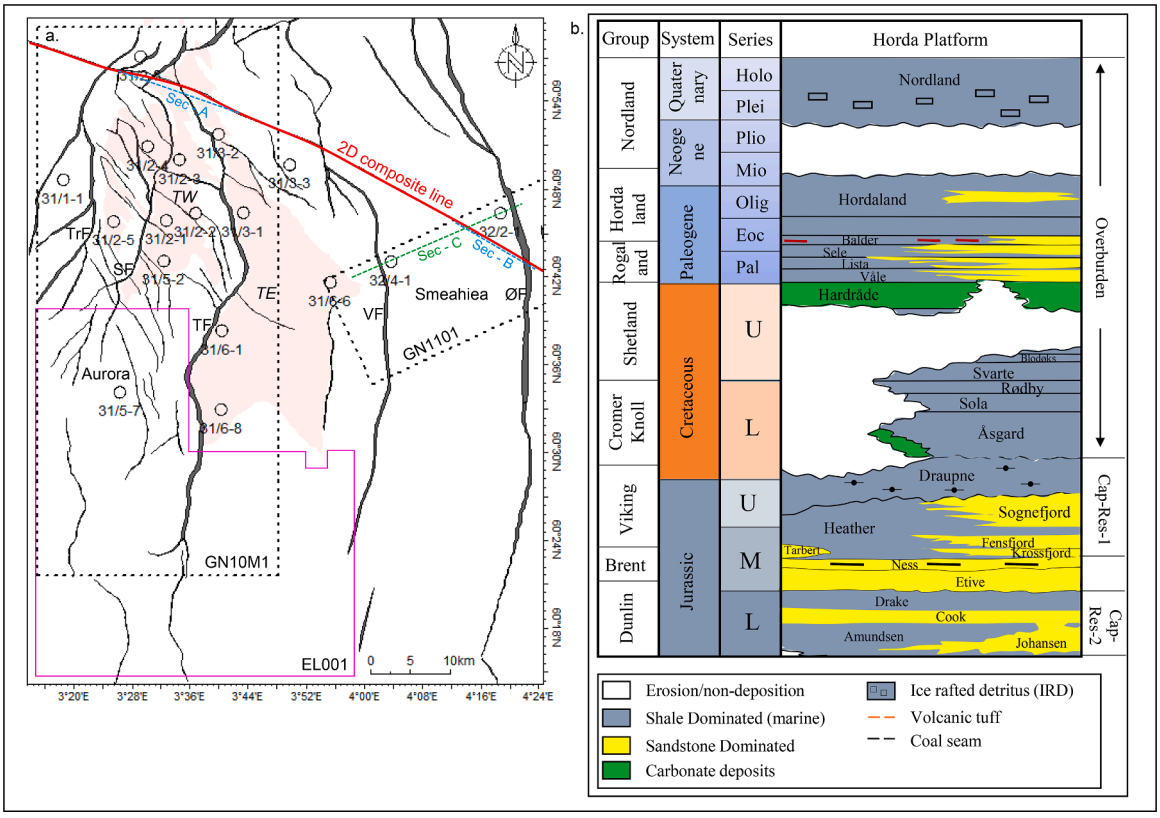

Fig. 1. The map of the Horda Platform area shows the potential CO_2 storage sites - Aurora and Smeaheia. The North-South Trending major faults (ØF – Øygarden Fault; VF – Vette Fault; TF – Tusse Fault; SF – Svartalv Fault; TrF – Troll Fault) and several minor faults are illustrated as black lines. The black dotted rectangle represents the 3D seismic cubes in Smeaheia (GN1101) and Aurora (GN10M1) areas. The CCS license boundary (EL001), exploration wells, and Troll Fields (i.e., TE – Troll East and TW – Troll West) are also presented as references. The red line represents a 2D seismic composite line, and two blue dashed lines (*sec*. A and Sec. B) are random lines taken from the GN10M1 and GN1101, respectively. Another random line from GN1101 (green dashed line) is used for detailed characterization of the Smeaheia injection site.

(Anell et al., 2012; Jordt et al., 2000; Rundberg, 1989). Within the Hordaland and Rogaland Groups, there is evidence of a polygonal fault system that developed during the post-rift phase from the Early Pliocene to the Middle Miocene. These faults terminate at the top of the Hordaland Group, which is marked by a mid-Miocene unconformity resulting from either non-deposition or erosion processes that occurred over approximately 10 million years (Løseth et al., 2013; Wrona et al., 2017).

These faults are layer-bounded, low-displacement (<100 m throw), normal faults with a polygonal arrangement and occur within fine-grained sedimentary successions (such as shales). To evaluate the creation of the polygonal fault system, many different mechanisms have been proposed (Henriet et al., 1988; Watterson et al., 2000; Clausen et al., 1999; Higgs and McClay, 1993; Cartwright, 1994a, 1994b; Dewhurst et al., 1999; Goulty, 2008, 2001; Goulty, 2001; Cartwright, 2011; Shin et al., 2008; Laurent et al., 2012) but the exact driving force to develop these fault systems remains unclear. Because of the potential influence of polygonal fault systems on secondary sealing capacity, it is critical to evaluate the distribution and sealing potential of these faults. Additionally, investigating how these faults might impact the secondary seal is vital in both injection sites.

3. Materials and methods

3.1. Seismic interpretation and attributes analysis

Nine overburden horizons and major and minor faults have been interpreted in a 2D composite line and two 3D seismic cubes (GN1101 and GN10M1) to investigate the overburden intervals. In addition, the Aurora site seismic cube (GN10M1) has been evaluated for possible hydrocarbon leakage from the Troll West field and accumulations within the overburden intervals. The surfaces interpreted using 3D cubes have also been used for extracting attribute properties to assess lateral distributions of migrated hydrocarbon.

Seismic attributes serve as valuable tools for assessing subsurface geometry and physical characteristics. These attributes are derived from elastic properties, such as acoustic impedance, reflection coefficient, velocities, and absorption. Analyzing seismic attributes makes it possible to quantify the properties of rocks and fluids, as there is a relationship between these parameters and geological patterns and features, including structural configuration, lithological variation, and fluid content (Chopra and Marfurt, 2005). Both pre-stack and post-stack seismic data can be utilized to generate these attributes. However, the focus of this study is solely on post-stack attributes, which are generated using the Petrel-2021 volume attribute function. This approach allows for a comprehensive analysis of the subsurface, enabling insights into the geological properties and their spatial variations. We used the 3D seismic cubes from the Smeaheia (GN1101), and Aurora (GN10M1) sites for attribute analysis. Due to stacking processes, post-stack attributes have limitations(i.e., they do not provide offset and azimuth-related information); however, they are suitable for initial reconnaissance investigations enabling us to observe large amounts of data (Taner, 2001).

One of the seismic attributes, called variance, measures the variation in seismic amplitudes within a seismic volume and can be used to identify subtle changes in amplitudes due to the presence of faults and fractures. The variance property is estimated using the default filter (i.e., 3, 3, 15 - inline, crossline number of traces, and vertical smoothing). This

study used the post-stack variance attribute to identify faults and fracture zones within the overburden intervals. We compared our analysis to other available data(e.g., seismic interpreted faults) in order to validate our findings using the variance attribute. Another post-stack attribute, sweetness, is used to identify possible gas leakage and accumulation within the overburden intervals. The seismic sweetness attribute is a measure of the amplitude of seismic reflections, which could be related to the presence of hydrocarbon fluids.

3.2. Brittleness indices

Overburden interval brittleness indices (BI) property has been evaluated using two elastic properties based (EBI) empirical equations. Seismic inverted property cubes have been converted and analyzed for spatial and vertical variations. The first equation is based on normalizing Young's modulus and Poisson's ratio (Grieser and Bray, 2007; Rickman et al., 2008) and states that:

$$EBI^1 = \frac{1}{2}\left[\frac{E_s - E_{\min}}{E_{\max} - E_{\min}} + \frac{\nu - \nu_{\max}}{\nu_{\min} - \nu_{\max}}\right], \quad (1)$$

where E_s is static Young's modulus, and ν is static Poisson's ratio. Also, the higher the EBI^1 value is, the more brittle the caprock is. Young's modulus and Poisson's ratio cubes for Smeaheia 3D (GN1101) have been extracted using the pre-stacked seismic inverted cubes (Fawad et al., 2021b, 2021a).

The other elastic BI equation proposed by Fawad and Mondol (2021) is based on acoustic impedance (AI) and deep resistivity (R_t) and is defined as:

$$EBI^2 = \frac{0.00044AI - 1.3 - \sqrt{0.62\ \frac{R_w}{R_t}}\,(0.00019AI + 0.25)}{1.35\ +\ 0.00028AI}, \quad (2)$$

where AI is the acoustic impedance (m/s × g/cm^3), R_D and R_W are the resistivities of true formation and pore water, respectively, in ohm-m. The brittleness value is defined as an increase in the stiffness of rock by adding stiff mineral content (i.e., quartz, calcite, or dolomite). AI cube has been estimated using the pre-stack inversion (Fawad et al., 2021a, 2021b), while $\sqrt{\frac{R_w}{R_t}}$ of a water-matrix system is calculated using the equation below (Fawad and Mondol, 2021):

$$\sqrt{\frac{R_w}{R_t}} = \frac{\rho_{ma} - \frac{AI}{Vp_{ma}}}{\sqrt{a}\left[AI\left(\frac{1}{Vp_w} - \frac{1}{Vp_{ma}}\right) - (\rho_w - \rho_{ma})\right]}, \quad (3)$$

where water density (ρ_w) and velocity (Vp_w) are used as 1.1 g/cm^3 and 1480 m/s and quartz matrix density (ρ_{ma}) and velocity (Vp_{ma}) are 2.65 g/cm^3 and 6000 m/s. In addition, the tortuosity factor (a) is used as 0.62.

3.3. Structural reliability analysis

The structural reliability of polygonal fault systems has been evaluated. The reliability of any structure depends on the active load (S) and resistance (R) and can be determined by the following equation:

$$P_f = \Phi\left(\frac{0 - \mu_M}{\sigma_M}\right) = \Phi(-\beta) \quad (4)$$

Where the probability of failure is P_f and the reliability/safety index is β. The limit state function (g(x)) can be used to estimate the probability of failure (P_f) of any structure by defining the boundary between desired (g(x)>0) and undesired (g(x)≤0) performance (Ditlevsen and Madsen, 2007).

Mohr-Coulomb failure criteria-based limit state function for structural reliability assessment has been introduced for subsurface by Rahman et al. (2021), where g(x) can be determined from the deterministic factor of safety (FoS) equation. To make the model simple, an isotropic horizontal stress condition with a normal faulting regime has been assumed. The factor of safety (FoS) for shear failure can be expressed mathematically as:

$$FoS = \frac{\tau_{MC}}{\tau_{current}} \quad (5)$$

$$\tau_{MC} = S_o + \sigma_n^{'} \cdot tan\varnothing \quad (6)$$

$$\tau_{current} = \frac{\sigma_1^{'} - \sigma_3^{'}}{2} \cdot sin2\theta \quad (7)$$

$$\sigma_n^{'} = \frac{\sigma_1^{'} + \sigma_3^{'}}{2} + \frac{\sigma_1^{'} - \sigma_3^{'}}{2} \cdot cos2\theta \quad (8)$$

where τ_{MC} is critical shear stress or shear strength, $\sigma_n^{'}$ is effective normal stress, S_o is cohesion, σ_1 is initial vertical stress, σ_3 is initial horizontal stress, $\sigma_1^{'}$ is effective vertical stress, $\sigma_3^{'}$ is effective horizontal stress, $\varnothing$ is an effective friction angle, and θ is fault dip.

According to the FoS, the structure will be safe if the FoS value is > 1 and fails if it is ≤1. The mathematical expression of that is:

$$g(x) = FoS - 1 \quad (9)$$

Hasofer and Lind (1974) proposed FORM (First Order Reliability Method) technique has been used to run the model for estimating structural reliability (Faber, 2009; Nadim, 2007). According to this method, the reliability index (β_{HL}) is the shortest distance z* from the origin to the failure surface g(z) in a normalized space.

Based on the fault plane rock cohesions (Wrona et al., 2017), two different scenarios such as cohesionless and cohesive clay as fault rock, have been tested (Table 1). For case-1, the side-wall cores-based cohesion property estimated from the triaxial laboratory test has been adapted from Wensaas et al. (1998). A standard cohesionless fault friction angle (31°) is used for case-2. Table 2 represents the average and standard deviation of all the input data used for polygonal fault structural reliability analysis. The fault stability assessment is focused on 800 m depth below the seafloor. Therefore, the in-situ stresses are estimated based on Gassnova (2012) report on that specific depth (Rahman et al., 2021; 2022a). Moreover, a large part of the Norwegian North Sea

Table 1
The different model scenarios are tested in this study to evaluate the polygonal fault system's reliability.

	Unit	Assumptions
Case-1	Hordaland Group	Cohesive clay from triaxial testing from side-wall cores
Case-2		Cohesionless fault system

Table 2
Input parameters for the model with the type of distribution and data sources.

Parameters	Average (unit)	Standard Deviation	Random Distribution	Data Source
Initial vertical stress (σ_v)	11.39 (MPa)	0.65	Normal	Gassnova, 2012
Initial horizontal stress (σ_h)	9.08 (MPa)	0.95	Normal	Gassnova, 2012
Initial pore pressure (P_p)	8.04 (MPa)	1.32	Normal	Gassnova, 2012
Fault Dip (θ)	35(°)	5.00	Normal	Wrona et al., 2017
Cohesionless (ϕ)	31 (°)	0.00	–	–
Cohesion (S_o)	1.1 (MPa)	1.62	Normal	Wensaas et al., 1998
Friction angle (ϕ)	17 (°)	2.27	Normal	Wensaas et al., 1998

exhibits pore pressure close to hydrostatic. This study also considers hydrostatic pore pressure within overburden intervals. Additionally, polygonal fault rock properties are scouted from Wensaas et al. (1998), and fault dip from Wrona et al. (2017).

4. Results

4.1. Troll field leakage and polygonal fault systems

The overburden intervals above the Sognefjord reservoir sandstone are the main zone of interest for this study (Fig. 1b), where nine different layers have been interpreted from the Viking, Cromer Knoll, Shetland, Rogaland, Hordaland and Nordland Groups (Fig. 2). Three major faults such as Øygarden, Vette and Tusse are present which are located from east to west, respectively. Overburden layers are dipping towards the west and are truncated by Middle Miocene Unconformity (MMU) in the east.

The Troll Field has been divided into east and west by the Tusse fault (Fig. 2b). Several other faults also penetrate through the reservoir and further down. Sets of minor small-scale faults, which are called polygonal fault systems, are also present within the Rogaland and Hordaland Group intervals. In the 2D composite section (Fig. 2a), the primary caprock for the Troll Field Draupne shale was either eroded by the Base Cretaceous Unconformity (BCU) or was not deposited due to uplift (Fig. 2; Rahman et al., 2020). If we see the zoomed 3D seismic random line from the GN10M1 section (Fig. 2b) with the same orientation as the 2D composite line, a high amplitude region within the overburden just above the Troll Fields can be observed. These high amplitude areas possibly indicate fault parallel hydrocarbon leakage from the Troll. The escaped hydrocarbon possibly gathered within the overburden interval as a secondary accumulation (Fig. 2b). Although the Tusse fault in this area has a low fault throw, no primary Draupne shale could influence the fault parallel leakage. Moreover, the polygonal fault systems within the Rogaland and Hordaland Groups might also act as conduits, leading to the Troll hydrocarbon fluids migrating upward.

To find out the conformity of the fracture zone parallel to fluid flow and possible secondary accumulation, variance and sweetness attributes of the same section have been illustrated in Fig. 3. Most faults interpreted on seismic are aligned with high variance anomalies (Fig. 3a). Moreover, the possible leakage pathways show vertically connected fracture zones in both the Tusse fault and other minor fault paths (Fig. 3a). Additionally, hydrocarbon that possibly leaked from the Troll field and subsequently accumulated within the overburden intervals can be identified by the sweetness attribute. The high sweetness values within the overburden and Troll field confirm the relationship between hydrocarbon and the sweetness attribute (Fig. 3b). However, the other high sweetness anomalies in the area might well be formed because of high acoustic impedance contrast due to lithology variation such as organic-rich Draupne shale and Opal-A/CT alternative layers.

The leakage scenario in the Troll field indicates that the polygonal fault system present within the Rogaland and Hordaland Groups might not be sealed and allow fluid to flow parallel to the fault planes. However, the ductile clay within the overburden interval may act as an impermeable secondary seal despite having polygonal faults present, trapping the fluid from moving further up. Also, the primary caprock (i.e., ductile Draupne shale) is not present in the leakage area.

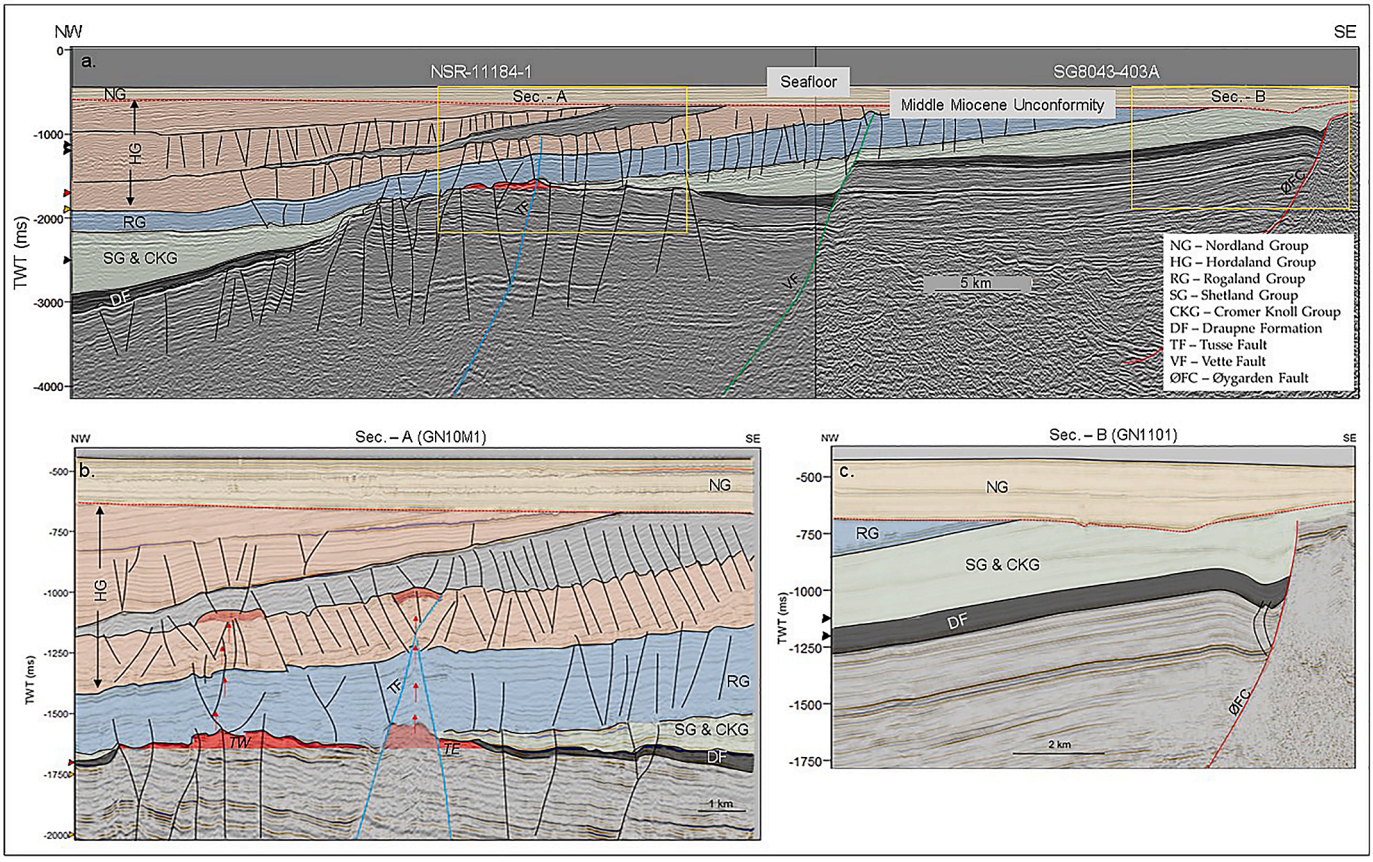

Fig. 2. The composite line consisting of NSR-11184-1 and SG8043-403A 2D seismic lines illustrate the interpreted major and minor faults and the different stratigraphic intervals (a), The same profile is also analyzed in random line (*sec*. - A) from the 3D seismic cube GN10M1 (b) and random line (*sec*. - B) from the 3D seismic cube GN1101 (c).

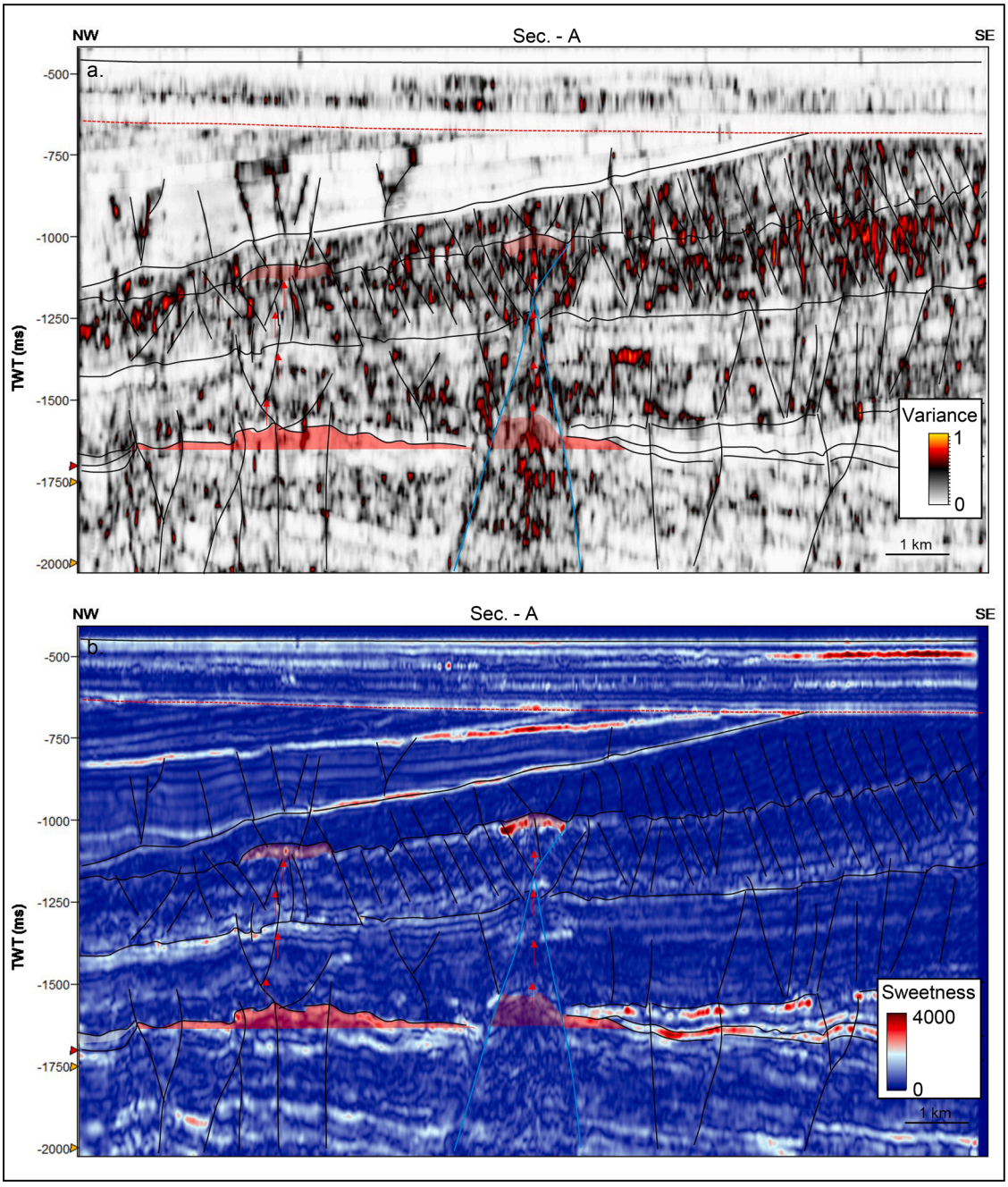

Fig. 3. The seismic attributes variance (a) and sweetness (b) are presented in the random line (*sec*. - A) with the interpreted faults. The possible leakage paths from Troll West are illustrated.

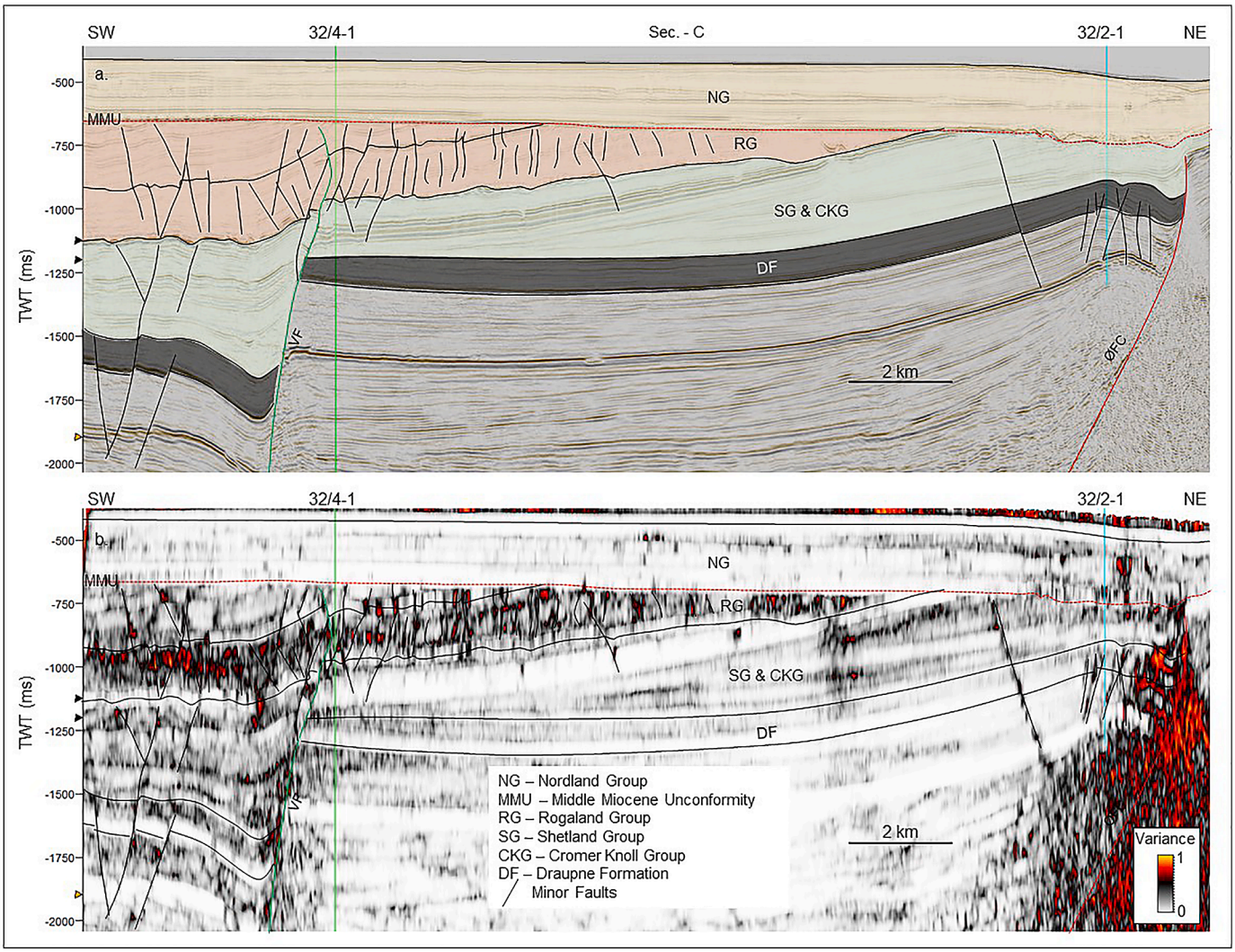

Fig. 4. The interpretation of the overburden stratigraphic intervals and faults on post-stack seismic section (Sec. – c in Fig. 2) over the Alpha and Beta structures (a). The seismic attribute variance (b) is presented in the same section with the interpreted faults.

4.2. Polygonal faults in Smeaheia area

The potential storage site Smeaheia is located further east from the Troll field, bounded by the Vette fault in the west and Øygarden fault in the east (Fig. 1). Due to the truncation of overburden layers by MMU (Fig. 4), most of the Hordaland Group layers with polygonal fault systems are not present in the Smeaheia area. Instead, a faulted Rogaland Group interval (i.e., Lista Formation) is present with a different fault orientation and configurations compared to the Hordaland polygonal fault system in the Aurora area (Fig. 4a). Additionally, the Lista Formation is truncated by MMU in the middle of the Smeaheia area. The variance attribute also confirms the faults by exhibiting high variance anomalies (Fig. 4b). The basement (east of Øygarden fault) is also highly fractured, as indicated by the variance attribute.

4.3. Overburden geomechanical properties

Rock failure is dependent on the brittle behavior of the rock. Therefore, the overburden rock brittleness in the Smeaheia site has been evaluated using two elastic property-based empirical equations (Eqs. (1) and (2)). Both methods indicated comparatively higher brittleness indices (BI) values within the faulted Lista Formation than the other overburden layers. The BI values change slightly between the different approaches; however, the lateral and vertical trends of BI are similar (Fig. 5).

4.4. Polygonal faults failure potential

Possible hydrocarbon leakage from the Troll Field through faults indicates fault-parallel flow. This implies that the polygonal fault systems within the overburden intervals are non-sealing up to the secondary ductile shale layers, where the migrated fluids accumulate instead of escaping to the surface. The structural reliability analysis also reveals that the studied polygonal faults have very high failure numbers, whereas the cohesive fault properties case has 36% failure risks with a 0.34 reliability index value (Table 3). Additionally, the cohesionless scenario has doubled the failure number with 65% and a negative reliability index. According to the U.S. Army Corps of Engineers (1997), these values are above the riskiest case, called hazardous, with a PoF of 0.16 and a reliability index of 1. Rahman et al. (2022c) also proposed

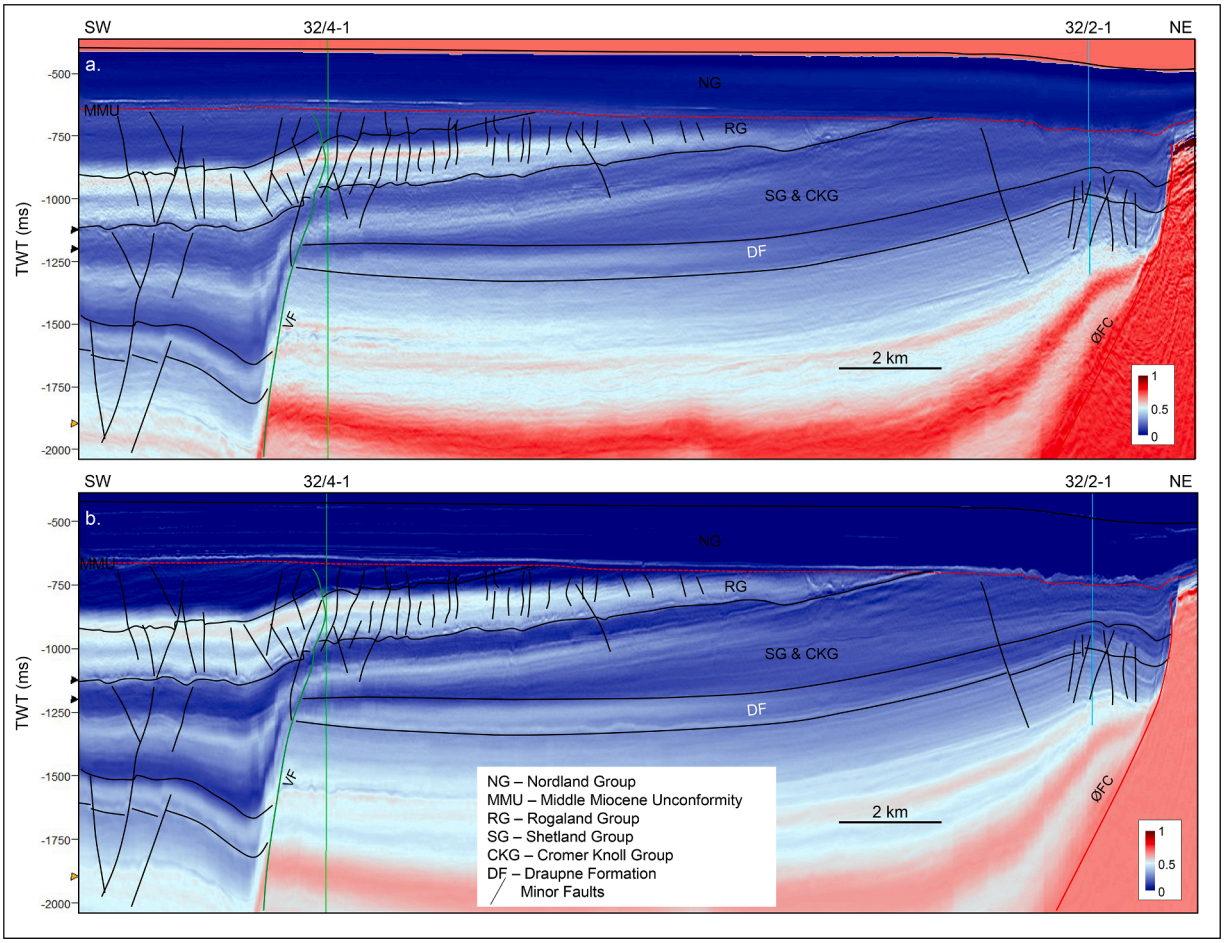

Fig. 5. The elastic property-based brittleness indices illustrate the lateral and vertical changes of brittleness indices values. (a) BI estimated using Young's modulus and poisson's ratio (Grieser and Bray, 2007; Rickman et al., 2008), and (b) BI estimated using Acoustic Impedance and deep resistivity (Fawad and Mondol, 2021).

Table 3
Probability of failure and reliability index of polygonal fault system for various cases.

	PoF	β
Case-1	0.3638	0.3484
Case-2	0.6588	−0.4093

this zone as unsatisfactory for subsurface structural reliability analysis. Moreover, the Vette fault probability of failure poses a very low number (1.46×10^{-04}) compared to the polygonal fault system (Rahman et al., 2021). Considering these, it seems the polygonal fault system might leak in the case of injection-induced fluid flow.

5. Discussions

The qualitative overburden study indicates that ductile secondary caprock is present within the Horda Platform area; in this respect, it covers the two CCS license numbers EL001 and EL004. The ductile shale in the Smeaheia area (EL002), however, has been eroded by the Middle Miocene Unconformity (MMU). The polygonal fault systems within the Rogaland and Hordaland Group intervals are unstable and have leaking potential, however, the ductile clay-rich unit may self-heal the faults, thereby trapping possible upward migrating fluids. This relationship between fault sealing and ductile clay-rich caprock has been observed in the Troll field leakage pathways. Further to this, in-depth studies of what drives the mechanical properties of the caprock would seem to indicate this potential (Johnson et al., 2022a, 2022b). The Tusse fault leakage is concentrated only in the northernmost part of the fault segment where the throw is comparatively low, and no primary caprock (ductile clay-rich Draupne formation shale) is present due to erosion or non-deposition (Fig. 2). No leakage through the rest of the Tusse fault section is inferred where there is high clay smear potential showing a safe structural closure with no leakage pathways. The accumulation of hydrocarbon leaked from the Troll structure within the ductile secondary caprock also proves the faults self-sealing potential when the clay-rich interval is present. Additionally, this fault's self-sealing potential could be crucial during injection-induced seismicity. If a fault is re-activated due to possible seismicity, it may heal itself thereafter if a ductile clay-rich unit is present. There are many other processes involved in fault dynamics, but the presence of ductile clay should enhance the sealing potential of a fault under in-situ stress conditions (Vrolijk et al., 2016; Johnson et al., 2022b, 2022d).

The possible leakage scenarios in Smeaheia and Aurora injection sites are theoretical and have been analyzed based on the Troll field leakage analogue and overburden analysis. However, to have a realistic scenario, we need numerical simulation coupling between fluid flow and geomechanical modeling, which is out of the scope of this work. Such modeling, while not directly applied to the site, has been carried out from a first principles perspective by other groups (Panahi et al., 2013; Kobchenko et al., 2013; Yarushina et al., 2020; Johnson et al., 2022c). This study qualitatively assesses the consequences for the Aurora and

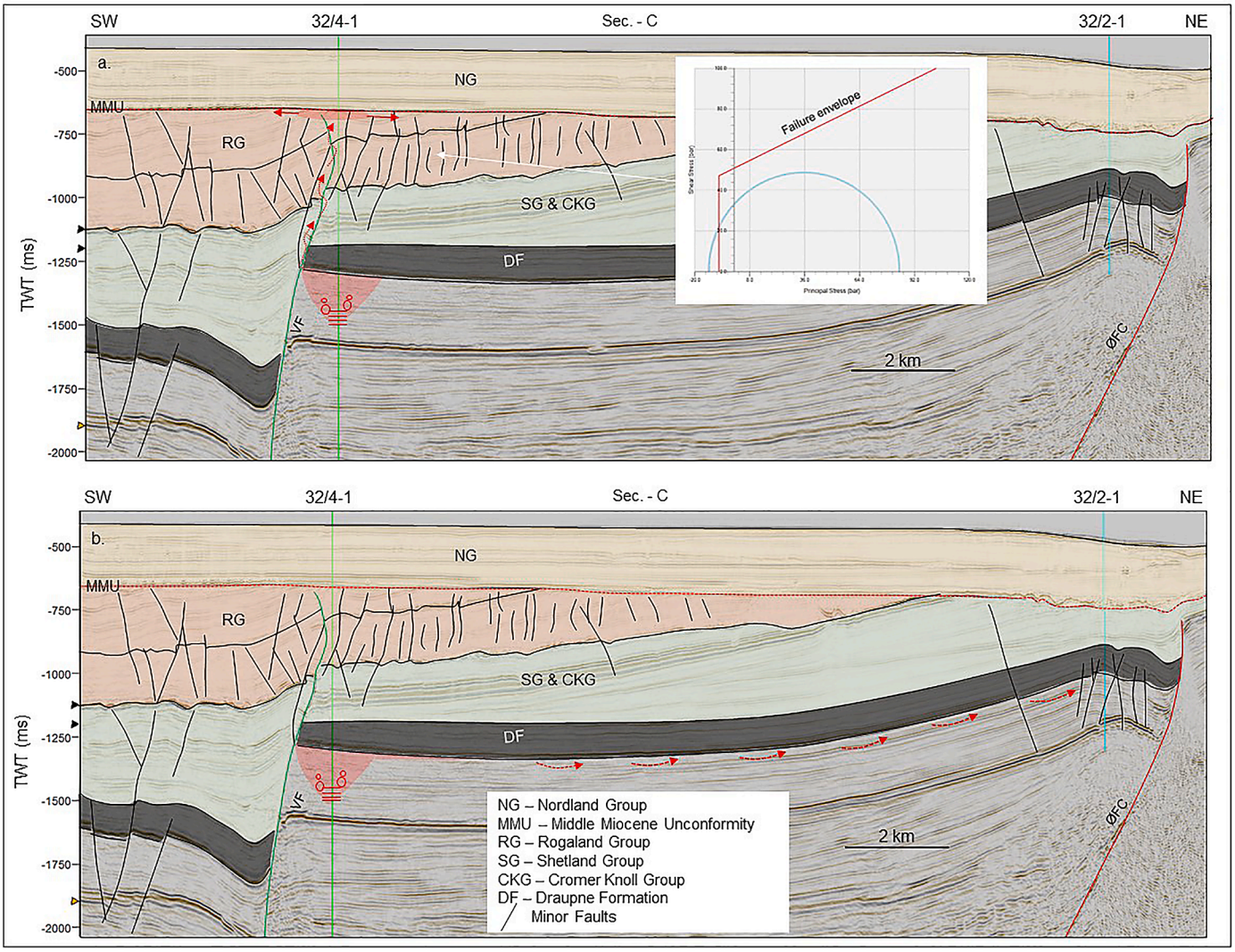

Fig. 6. Two possible CO_2 injection scenarios in Alpha structure at Smeaheia site (a) if Vette fault leaks (b) sealing Vette fault but fluid migrated to up-dip Beta structure. The inset figure is the Mohr-Coulomb failure plot of the Lista Formation layer, indicating tensile failure potential adapted from the numerical simulation by Rahman et al. (2022a).

Smeaheia injection sites, considering different theoretical failure scenarios.

5.1. *Smeaheia CO_2 injection site (EL002)*

The Vette fault in the Alpha structure (32/4-1 well location) could be impermeable under in-situ stress conditions with very low failure potential (Rahman et al., 2021). However, there is the possibility of reactivation due to injection-induced seismicity, as many faults in the North Sea are critically stressed (Grollimund and Zoback, 2003). The primary caprock, i.e., Draupne Formation shale, is clay-rich, ensuring a sealing Vette fault under in-situ stress conditions. Nevertheless, the possible theoretical failure of the Vette fault due to injection-induced seismicity has been considered here to assess the integrity of overburden secondary caprocks and faults. In the case of a leaking Vette fault, injected CO_2 might migrate upward to the Middle Miocene Unconformity (MMU), because of the structurally unstable polygonal fault system (Fig. 6a). Due to high brittleness in the Lista formation, our geomechanical simulation model indicates potential stress-induced tensile failure at 32/4-1 (inset picture on Fig. 6a; Rahman et al., 2022a), which unfortunately also aligns with the polygonal fault systems within this interval. The migrated CO_2 plume might change from supercritical to gas phase because of shallowing depth (i.e., decreased temperature and pressure). From this point, the plume could migrate laterally as the top of the Nordland Group shale has demonstrated sealing quality as an effective caprock for the Sleipner CO_2 injection site. If this scenario occurs, there is a possibility that the CO_2 plume will migrate laterally updip below the MMU. This migration will take place at a comparatively quicker pace due to phase change.

In another scenario, there could be no leakage from the Vette fault, but the injected volume in the Alpha structure is accumulated down to the spill point and starts migrating eastward to the Beta structure (32/2-1), which is located on the hanging wall side of the Øygarden fault and juxtaposes with bedrock (Fig. 6b). This structure is highly faulted, but most of faults die out within the Draupneand Åsgard shale. Because of the shaly intervals, these faults may self-heal, and provide an effective seal in Beta structure.

As the uppermost Nordland shale is vital in case of any leakage from the Smeaheia reservoir, three slices of extracted variance attribute have been evaluated within this zone (Fig. 7). The variance attribute was extracted on the top of three interpreted surfaces. The interpreted surfaces are the seafloor, the middle of Nordland (100 ms below the

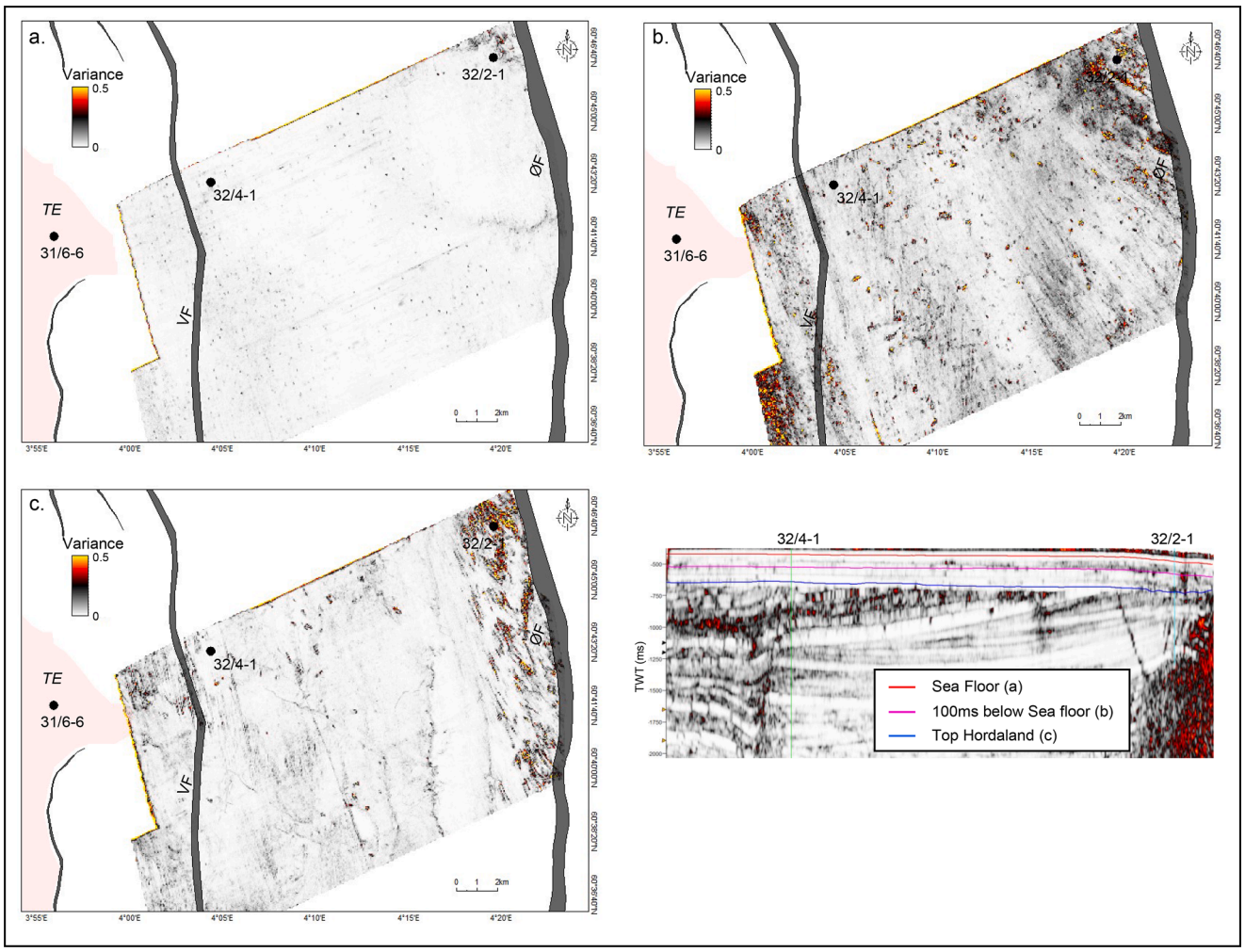

Fig. 7. Top view of variance attribute illustrates the possible fracture zones in the Smeaheia CO_2 injection site; average variance properties are extracted on top of the seafloor (a), 100 ms below seafloor (b), and Middle Miocene Unconformity (c). The major faults (ØF – Øygarden fault and VF – Vette fault) and 32/4-1 (Alpha), 32/2-1 (Beta), and 31/6-6 (Troll East) wells are also illustrated for reference.

seafloor), and the Middle Miocene Unconformity. The top of the seafloor shows a few points anomalies with high variance, indicating seafloor pockmarks. However, seafloor pockmarks are not randomly distributed; instead, they follow an NW-SE trend, one in the middle of the Smeaheia and another following the Vette fault (Fig. 7a). Although the variance attribute does not indicate any possible fault or fracture, spectral decomposition attribute analysis represents a weak fault trace south of Alpha structure (Fawad and Mondol, 2019). Additionally, a fracture zone with a high variance value is present near 32/2-1 (Beta) well. The pockmarks are more prominent in the middle of the Nordland shale compared with the seafloor, containing larger circles that are randomly distributed (Fig. 7b). Moreover, a possible fracture zone on top of the Beta structure extends further south. Only a few pockmarks are observed on top of the MMU surface. However, the Beta structure fracture zone extends throughout the seismic coverage and follows the Øygarden fault orientation (Fig. 7c).

Considering the qualitative risk assessment in the Smeaheia overburden interval, it is recommended that the Beta structure needs extensive analysis before any injection decision. In the Alpha structure, the optimum capacity and injectivity rate need to be estimated so that the Vette fault will not reactivate due to injection-induced pressure buildup. The Alpha structure should also not be filled up to the spill point level.

5.2. *Aurora CO_2 injection site (EL001)*

Although the polygonal fault systems are present within the Hordaland and Rogaland Groups, the overburden intervals in the Aurora site differ significantly from Smeaheia because the reservoirs here are the Late Jurassic Cook and Johansen formation sandstones (Fig. 1). The thick, primary caprock shale of the Drake formation has no major faults close to the injection points. The Brent Group intervals are also present between the Drake shale and the Troll field reservoir units of Viking Group. Reservoir pressure data acquired in 2020 through the Eos well, indicates no fluid communication between depleted Viking sandstones and the underlying sandstones of the Brent and Dunlin groups (Fig. 8). The Viking reservoir sandstones with their current pressure depletion of ~1–3 MPa (Rahman et al., 2022b) due to Troll west production, do not seem to be connected with the Brent and Dunlin sandstones as they exhibit hydrostatic pressure. However, injection-induced seismicity could reactivate existing faults and connect the overlying depleted and the underlying pressurized sandstones. A coupled fluid flow and geomechanical simulation can model these scenarios, which might be required to estimate the Aurora injection site's optimum capacity and injectivity rate.

Chances of caprock shale failure are minimal because of the thick Drake shale present throughout the area with high top seal reliability (Rahman et al., 2022b). Considering the faults as the only fluid

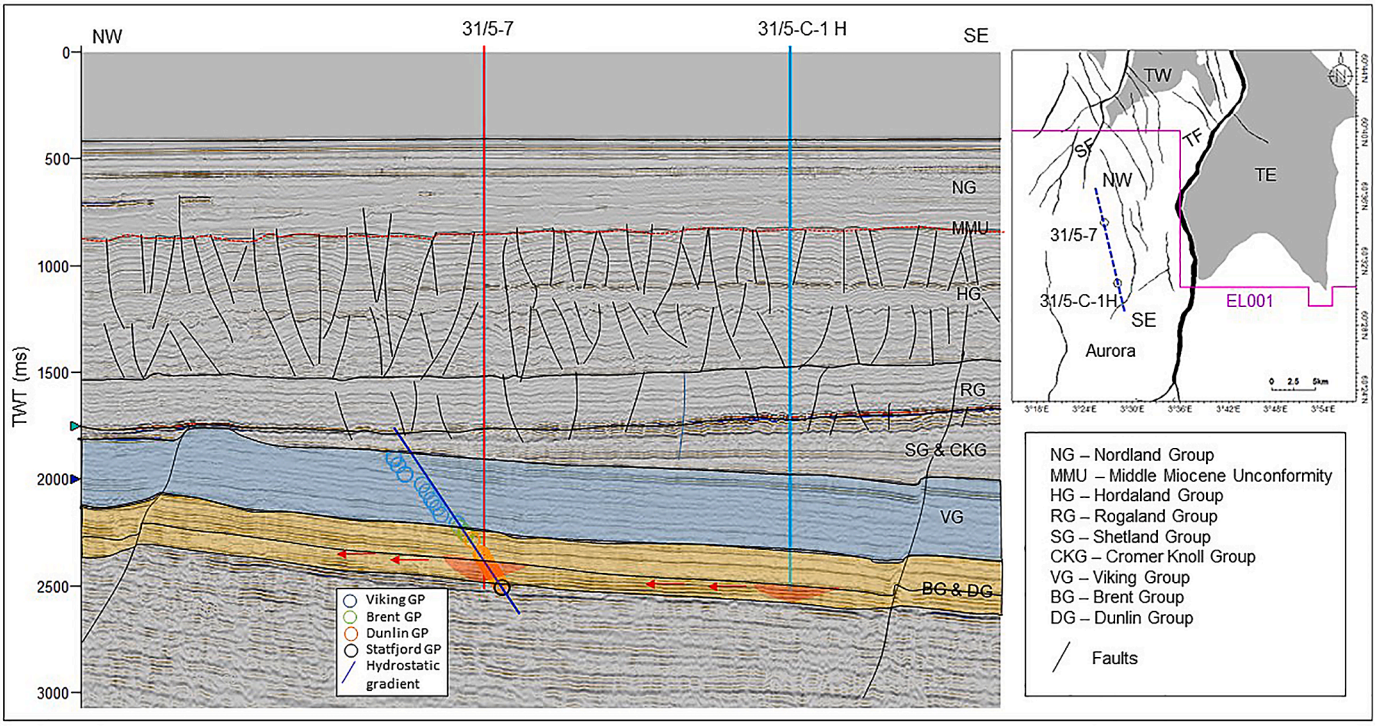

Fig. 8. N-S random line from GN10M1 illustrated faults and lithological intervals in the Aurora injection site. Recently drilled injection wells are also present where the possible CO_2 plume migration paths are shown. Also, the reservoir pressure data of the Eos (31/5-7) well is displayed for reference.

migration pathways, the CO_2 plume would laterally migrate a long distance with a very gentle slope (2–3° bedding dip towards the south). Considering the plume travel time from the injection point to a leaking fault (if any) and the corresponding years of Troll West production, this scenario might benefit the Aurora injection site. Instead of being impacted negatively, the connectivity between depleted and pressurized reservoirs might allow more storage opportunities. However, a numerical coupled model must simulate and test different scenario-based sensitivities to quantify it.

It is improbable that the CO_2 plume will migrate further upward from the depleted reservoirs to the Rogaland and Hordaland groups. However, if leakage occurs, we know that there is an effective secondary top seal, which accumulated Troll field leakage (Fig. 2), present to stop further fluid migration.

6. Conclusions

The key findings from this research are:

- Accumulation of hydrocarbons over the Troll field indicates the presence of a secondary caprock within the Hordaland Group intervals in EL001 and EL004 license locations.
- Polygonal fault systems are present within the Rogaland and Hordaland groups interval and cover the entire study area. However, the fault frequency and orientation vary between Rogaland and Hordaland layers.
- Polygonal fault systems are not structurally stable, indicating possible fault parallel leakage pathways.
- Clay-rich shale could potentially heal the faults and stop fluid from migrating upward.
- The stability of the Vette fault and Nordland Group shale caprock potential are the critical parameters for the reliability of the Smeaheia injection site.
- For the Aurora site, connectivity between depleted and pressurized reservoirs is critical. However, under in-situ stress conditions, the pore pressure in well 31/5-7 (Eos) indicates no connectivity.

According to this qualitative assessment, we can conclude that the overburden interval in the Horda platform area has a secondary sealing potential to hold and accumulate if CO_2 escapes from the reservoirs due to the primary seal failure. However, a numerical simulation in both the Aurora and Smeaheia sites is recommended to quantify the findings.

CRediT authorship contribution statement

Md Jamilur Rahman: Writing – review & editing, Writing – original draft, Visualization, Validation, Software, Methodology, Investigation, Formal analysis, Data curation, Conceptualization. **Manzar Fawad:** Writing – review & editing, Validation. **Nazmul Haque Mondol:** Writing – review & editing, Validation, Supervision, Project administration, Funding acquisition.

Declaration of competing interest

The authors declare that they have no known competing financial interests or personal relationships that could have appeared to influence the work reported in this paper.

Data availability

Data will be made available on request.

Acknowledgments

We express our gratitude for the generous financial support from the Research Council of Norway for the OASIS (Overburden Analysis and

Seal Integrity Study for CO_2 Sequestration in the North Sea) project (NFR-CLIMIT project #280472). We want to acknowledge the invaluable contributions of the Norwegian Petroleum Directorate (NPD), Gassnova, Equinor, and TotalEnergies, who provided additional funding and essential data for this study. We are also grateful for the academic software licenses granted by Lloyd's Register and SLB for Interactive Petrophysics and Petrel, respectively. These software tools have played a crucial role in facilitating our research and analysis, allowing us to delve deeper into the study's objectives and achieve meaningful outcomes. Special thanks to James Johnson for his support in revising the manuscript. We are also grateful to the editors and reviewers for their constructive feedback and suggestions.

References

Abay, T.B., 2017. Diversity of Petroleum in terms of Source Rock Properties and Secondary Alteration Processes. A study of source rocks, migrated petroleum, oils and condensates from the Norwegian Continental Shelf. Ph.D. thesis. University of Oslo.

Anell, I., Thybo, H., Artemieva, I.M., 2009. Cenozoic uplift and subsidence in the North Atlantic region: geological evidence revisited. Tectonophysics 474, 78–105.

Anell, I., Thybo, H., Rasmussen, E., 2012. A synthesis of C enozoic sedimentation in the N orth S ea. Basin Res. 24, 154–179.

Cartwright, J., 2011. Diagenetically induced shear failure of fine-grained sediments and the development of polygonal fault systems. Mar. Pet. Geol. 28, 1593–1610.

Cartwright, J.A., 1994a. Episodic basin-wide hydrofracturing of overpressured early Cenozoic mudrock sequences in the North Sea Basin. Mar. Pet. Geol. 11, 587–607.

Cartwright, J.A., 1994b. Episodic basin-wide fluid expulsion from geopressured shale sequences in the North Sea basin. Geology 22, 447–450.

Chopra, S., Marfurt, K.J., 2005. Seismic attributes—a historical perspective. Geophysics 70, 3SO–28SO.

Clausen, J.A., Gabrielsen, R.H., Reksnes, P.A., Nysaether, E., 1999. Development of intraformational (Oligocene–Miocene) faults in the northern North Sea: influence of remote stresses and doming of Fennoscandia. J. Struct. Geol. 21, 1457–1475.

Dewhurst, D.N., Cartwright, J.A., Lonergan, L., 1999. The development of polygonal fault systems by syneresis of colloidal sediments. Mar. Pet. Geol. 16, 793–810.

Ditlevsen, O., Madsen, H.O., 2007. Structural Reliability Methods. John Wiley and Sons. Internet e. ed.

Dreyer, T., Whitaker, M., Dexter, J., Flesche, H., Larsen, E., 2005. From spit system to tide-dominated delta: integrated reservoir model of the Upper Jurassic Sognefjord Formation on the Troll West Field. In: Geological Society, London, Petroleum Geology Conference Series. Geological Society of London, pp. 423–448.

Faber, M.H., 2009. Basics of Structural Reliability. Swiss Fed. Inst. Technol. ETH, Zürich, Switz.

Færseth, R.B., 1996. Interaction of Permo-Triassic and Jurassic extensional fault-blocks during the development of the northern North Sea. J. Geol. Soc. London. 153, 931–944.

Faleide, J.I., Bjørlykke, K., Gabrielsen, R.H., 2015. Geology of the Norwegian continental shelf. Petroleum Geosciences: From Sedimentary Environments to Rock Physics, pp. 603–637.

Faleide, J.I., Kyrkjebø, R., Kjennerud, T., Gabrielsen, R.H., Jordt, H., Fanavoll, S., Bjerke, M.D., 2002. Tectonic impact on sedimentary processes during Cenozoic evolution of the northern North Sea and surrounding areas. Exhum. North Atl. Margin Timing, Mech. Implic. Pet. Explor. https://doi.org/10.1144/GSL.SP.2002.196.01.14.

Fawad, M., Mondol, M.D.N.H., 2021. Method for Estimating Rock Brittleness from Well-Log Data.

Fawad, M., Mondol, N.H., 2019. Geological and geophysical investigation of CO_2 storage site Smeaheia in the northern North Sea. SEG Technical Program Expanded Abstracts 2019. Society of Exploration Geophysicists, pp. 3285–3289. https://doi.org/10.1190/segam2019-3215406.1.

Fawad, M., Rahman, M.D.J., Mondol, N.H., 2021a. Seismic reservoir characterization of potential CO_2 storage reservoir sandstones in Smeaheia area, Northern North Sea. J. Pet. Sci. Eng. 205, 108812.

Fawad, M., Rahman, M.J., Mondol, N.H., 2021b. Seismic-derived geomechanical properties of potential CO_2 storage reservoir and cap rock in Smeaheia area, northern North Sea. Lead. Edge 40, 254–260.

Foschi, M., Cartwright, J.A., 2020. Seal failure assessment of a major gas field via integration of seal properties and leakage phenomena. Am. Assoc. Pet. Geol. Bull. 104, 1627–1648.

Gassnova, 2012. Geological storage of CO_2 from Mongstad. Interim report Johansen Formation.

Goulty, N.R., 2008. Geomechanics of polygonal fault systems: a review. Pet. Geosci. 14, 389–397. https://doi.org/10.1144/1354-079308-781.

Goulty, N.R., 2001a. Polygonal fault networks in fine-grained sediments–an alternative to the syneresis mechanism. First Break 19, 69–73.

Goulty, N.R., 2001b. Mechanics of layer-bound polygonal faulting in fine-grained sediments. J. Geol. Soc. London. 159, 239–246. https://doi.org/10.1144/0016-764901-111.

Grieser, W.V., Bray, J.M., 2007. Identification of production potential in unconventional reservoirs. In: Production and Operations Symposium. Society of Petroleum Engineers.

Grollimund, B., Zoback, M.D., 2003. Impact of glacially induced stress changes on fault-seal integrity offshore Norway. Am. Assoc. Pet. Geol. Bull. 87, 493–506.

Hasofer, A.M., Lind, N.C., 1974. Exact and invariant second-moment code format. J. Eng. Mech. Div. 100, 111–121.

Heggland, R., 1997. Detection of gas migration from a deep source by the use of exploration 3D seismic data. Mar. Geol. 137, 41–47.

Henriet, J.P., De Batist, M., Van Vaerenbergh, W., Verschuren, M., 1988. Seismic facies and clay tectonic features of the Ypresian clay in the southern North Sea. Bull. van Belgische Ver. voor Geol. 97, 457–472.

Higgs, W.G., McClay, K.R., 1993. Analogue sandbox modelling of Miocene extensional faulting in the Outer Moray Firth. Geol. Soc. London, Spec. Publ. 71, 141–162.

Holgate, N.E., Jackson, C.A.L., Hampson, G.J., Dreyer, T., 2015. Seismic stratigraphic analysis of the Middle Jurassic Krossfjord and Fensfjord formations, Troll oil and gas field, northern North Sea. Mar. Pet. Geol. 68, 352–380.

Ingram, G.M., Urai, J.L., Naylor, M.A., 1997. Sealing processes and top seal assessment. Norwegian Petroleum Society Special Publications. Elsevier, pp. 165–174.

Jackson, J.A., White, N.J., 1989. Normal faulting in the upper continental crust: observations from regions of active extension. J. Struct. Geol. 11, 15–36.

Johnson, J.R., Hansen, J.A., Rahman, M.J., Renard, F., Mondol, N.H., 2022a. Mapping the maturity of organic-rich shale with combined geochemical and geophysical data, Draupne Formation, Norwegian Continental Shelf. Marine Petrol. Geol. 138, 105525.

Johnson, J.R., Kobchenko, M., Mondol, N.H., Renard, F., 2022b. Multiscale synchrotron microtomography imaging of kerogen lenses in organic-rich shales from the Norwegian Continental Shelf. Int. J. Coal Geol. 253, 103954.

Johnson, J.R., Kobchenko, M., Johnson, A.C., Mondol, N.H., Renard, F., 2022c. Experimental modelling of primary migration in a layered, brittle analogue system. Tectonophysics 840, 229575.

Johnson, J.R., Bailey, A., Mondol, N.H., Renard, F., 2022d. Using microscopy image analysis to calculate the mineral brittleness index in organic-rich shale. In: EAGE 6th International Conference on Fault and Top Seals. EAGE, pp. 1–5.

Jordt, H., Faleide, J.I., Bjørlykke, K., Ibrahim, M.T., 1995. Cenozoic sequence stratigraphy of the central and northern North Sea Basin: tectonic development, sediment distribution and provenance areas. Mar. Pet. Geol. 12, 845–879.

Jordt, H., Thyberg, B.I., Nøttvedt, A., 2000. Cenozoic evolution of the central and northern North Sea with focus on differential vertical movements of the basin floor and surrounding clastic source areas. Geol. Soc. London, Spec. Publ. 167, 219–243.

Joy, A.M., 1993. Comments on the pattern of post-rift subsidence in the Central and Northern North Sea Basin. Geol. Soc. London, Spec. Publ. 71, 123–140.

Kobchenko, M., Hafver, A., Jettestuen, E., Galland, O., Renard, F., Meakin, P., Jamtveit, B., Dysthe, D., 2013. Drainage fracture networks in elastic solids with internal fluid generation. A Lett. J. Expplor. Front. Phys. 102, 66002.

Kyrkjebø, R., Kjennerud, T., Gillmore, G.K., Faleide, J.I., Gabrielsen, R.H., 2001. Cretaceous-Tertiary palaeo-bathymetry in the northern North Sea; integration of palaeo-water depth estimates obtained by structural restoration and micropalaeontological analysis. Norwegian Petroleum Society Special Publications. Elsevier, pp. 321–345.

Laurent, D., Gay, A., Baudon, C., Berndt, C., Soliva, R., Planke, S., Mourgues, R., Lacaze, S., Pauget, F., Mangue, M., 2012. High-resolution architecture of a polygonal fault interval inferred from geomodel applied to 3D seismic data from the Gjallar Ridge, Vøring Basin, Offshore Norway. Mar. Geol. 332, 134–151.

Leythaeuser, D., Radke, M., Schaefer, R.G., 1984. Efficiency of petroleum expulsion from shale source rocks. Nature 311, 745–748.

Leythaeuser, D., Schaefer, R.G., Yukler, A., 1982. Role of diffusion in primary migration of hydrocarbons. Am. Assoc. Pet. Geol. Bull. 66, 408–429.

Løseth, H., Raulline, B., Nygård, A., 2013. Late Cenozoic geological evolution of the northern North Sea: development of a Miocene unconformity reshaped by large-scale Pleistocene sand intrusion. J. Geol. Soc. London. 170, 133–145.

Mondol, N.H., Fawad, M., Park, J., 2018. Petrophysical analysis and rock physics diagnostics of Sognefjord Formation in the Smeheia area, Northern North Sea. In: 5th CO_2 Geological Storage Workshop, 21-23 November, Utrecht, the Netherlands. https://doi.org/10.3997/2214-4609.201802951.

Nadim, F., 2007. Tools and strategies for dealing with uncertainty in geotechnics. Probabilistic Methods in Geotechnical Engineering. Springer, pp. 71–95.

NPD, 2023. NPD FactPages [WWW Document]. URL. https://npdfactpages.npd.no/factpages/Default.aspx?culture=en.

NPD CO2 Atlas, 2014. NPD CO2 Atlas Report.

Panahi, H., Kobchenko, M., Renard, F., Mazzini, A., Scheibert, J., Dysthe, D., Jamtveit, B., Mathe-Sorenssen, A., Meakin, P., 2013. A 4D synchrotron x-ray-tomography study of the formatioon of hydrocarbon-migration pathways in heated organic-rich shale. SPE J. 18 (2), 366–377.

Rahman, M.J., Choi, J.C., Fawad, M., Mondol, N.H., 2021. Probabilistic analysis of Vette fault stability in potential CO2 storage site Smeaheia, offshore Norway. Int. J. Greenh. Gas Control 108, 103315. https://doi.org/10.1016/j.ijggc.2021.103315.

Rahman, M.J., Fawad, M., Choi, J.C., Mondol, N.H., 2022a. Effect of overburden spatial variability on field-scale geomechanical modeling of potential CO2 storage site Smeaheia, offshore Norway. J. Nat. Gas Sci. Eng. 99, 104453.

Rahman, M.J., Fawad, M., Jahren, J., Mondol, N.H., 2022b. Top seal assessment of Drake Formation shales for CO_2 storage in the Horda Platform area, offshore Norway. Int. J. Greenh. Gas Control 119, 103700. https://doi.org/10.1016/J.IJGGC.2022.103700.

Rahman, M.J., Fawad, M., Mondol, N.H., 2020. Organic-rich shale caprock properties of potential CO2 storage sites in the northern North Sea, offshore Norway. Mar. Pet. Geol. 122, 104665.

Rahman, M.J., Fawad, M., Mondol, N.H., 2022c. Lateral Distribution of the Upper Amundsen Shale in Potential CO_2 Storage Site Aurora, Northern North Sea. Available SSRN 4284857.
Rahman, Md Jamilur, Fawad, M., Mondol, N.H., 2022d. Influence of rock properties on structural failure probability—caprock shale examples from the horda platform, offshore Norway. Energies 15, 9598.
Rahman, M.J., Johnson, J.R., Fawad, M., Mondol, N.H., 2022e. Characterization of Upper Jurassic organic-rich caprock shales in the Norwegian Continental Shelf. Geosci. (Basel) 12, 407.
Rickman, R., Mullen, M.J., Petre, J.E., Grieser, W.V., Kundert, D., 2008. A practical use of shale petrophysics for stimulation design optimization: all shale plays are not clones of the Barnett Shale. In: SPE Annual Technical Conference and Exhibition. Society of Petroleum Engineers.
Roberts, A.M., Kusznir, N.J., Yielding, G., Beeley, H., 2019. Mapping the bathymetric evolution of the Northern North Sea: from Jurassic synrift archipelago through Cretaceous–Tertiary post-rift subsidence. Pet. Geosci. 25, 306–321.
Roberts, A.M., Yielding, G., Kusznir, N.J., Walker, I., Dorn-Lopez, D., 1993. Mesozoic extension in the North Sea: constraints from flexural backstripping, forward modelling and fault populations. In: Geological Society, London, Petroleum Geology Conference Series. Geological Society of London, pp. 1123–1136.
Roberts, S., Jackson, J., 1991. Active normal faulting in central Greece: an overview. Geol. Soc. London, Spec. Publ. 56, 125–142.
Rundberg, Y., 1989. Tertiary History and Basin Evolution of the Norwegian North Sea between 60°-62° N—An Integrated Approach. Unpubl. Ph. D. Thesis. Univ. Trondheim.
Sales, J.K., 1997. AAPG Memoir 67: seals, traps, and the petroleum system. Chapter 5: Seal Strength vs. Trap Closure–A Fundamental Control On the Distribution of Oil and Gas.
Schowalter, T.T., 1979. Mechanics of secondary hydrocarbon migration and entrapment. Am. Assoc. Pet. Geol. Bull. 63, 723–760.
Schroot, B.M., Klaver, G.T., Schuttenhelm, R.T.E., 2005. Surface and subsurface expressions of gas seepage to the seabed - examples from the Southern North Sea. Mar. Pet. Geol. 22 (4), 499–515.
Shin, H., Santamarina, J.C., Cartwright, J.A., 2008. Contraction-driven shear failure in compacting uncemented sediments. Geology 36, 931–934.
Smith, J.E., Erdman, J.G., Morris, D.A., 1971. Migration, accumulation and retention of petroleum in the earth. In: 8th World Petroleum Congress. OnePetro.
Steel, R., Ryseth, A., 1990. The Triassic—Early Jurassic succession in the northern North Sea: megasequence stratigraphy and intra-Triassic tectonics. Geol. Soc. London, Spec. Publ. 55, 139–168.
Steel, R.J., 1993. Triassic–Jurassic megasequence stratigraphy in the Northern North Sea: rift to post-rift evolution. In: Geological Society, London, Petroleum Geology Conference Series. Geological Society of London, pp. 299–315.
Stewart, D.J., Schwander, M., Bolle, L., 1995. Jurassic Depositional Systems of the Horda Platform, Norwegian North Sea: Practical consequences of Applying Sequence Stratigraphic Models. Nor. Pet. Soc. Spec. Publ, pp. 291–323.
Taner, M.T., 2001. Seismic attributes. CSEG Rec. 26, 49–56.
U.S. Army Corps of Engineers, 1997. Engineering and Design Introduction to Probability and Reliability Methods for use in Geotechnical Engineering. Washington, D.C.
Vollset, J., Doré, A.G., 1984. A Revised Triassic and Jurassic lithostratigraphic Nomenclature for the Norwegian North Sea. Oljedirektoratet.
Vroilijk, P.J., Urai, J.L., Kettermann, M., 2016. Clay smear: review of mechanisms and applications. J. Struct. Geol. 86, 95–152.
Watterson, J., Walsh, J., Nicol, A., Nell, P.A.R., Bretan, P.G., 2000. Geometry and origin of a polygonal fault system. J. Geol. Soc. London. 157, 151–162. https://doi.org/10.1144/jgs.157.1.151.
Wensaas, L., Aagaard, P., Berre, T., Roaldset, E., 1998. Mechanical properties of North Sea Tertiary mudrocks: investigations by triaxial testing of side-wall cores. Clay Miner. 33 (1), 171–183.
Whipp, P.S., Jackson, C.L., Gawthorpe, R.L., Dreyer, T., Quinn, D., 2014. Normal fault array evolution above a reactivated rift fabric; a subsurface example from the northern Horda Platform, Norwegian North Sea. Basin Res. 26, 523–549.
Wrona, T., Magee, C., Jackson, C.A.L., Huuse, M., Taylor, K.G., 2017. Kinematics of polygonal fault systems: observations from the northern North Sea. Front. Earth Sci. 5, 101.
Yarushina, V.M., Podladchikov, Y.Y., Wang, L.H., 2020. Model for (de)compaction and porosity waves in porous rocks under shear stresses. J. Geophys. Res.: Solid Earth 125 (8), e2020JB019683.